Inhibiting $\sigma \rightarrow \pi$ Isomerization of Aryloxide Ligands in Late Transition-Metal Complexes

Jennifer L. Snelgrove, Jay C. Conrad, Melanie D. Eelman, Maeve M. Moriarty, Glenn P. A. Yap, and Deryn E. Fogg*

Centre for Catalysis Research and Innovation, Department of Chemistry, University of Ottawa, 10 Marie Curie, Ottawa, Ontario, Canada K1N 6N5

Received August 5, 2004

The room-temperature reaction of thallium perfluorophenoxide with $RuHCl(PPh_3)_3$ (**4a**) yields $RuH(\sigma\text{-}OC_6X_5)(PPh_3)_3$ (X = F, $\mathbf{5^F}$), the structure of which was confirmed by spectroscopic, microanalytical, and X-ray analysis. The analogous phenoxide complex (X = H, $\mathbf{5^H}$) is known to be unstable toward $\sigma \rightarrow \pi$ isomerization, and reaction of phenoxide ion with **4a** affords $RuH(\eta^5\text{-}C_6H_5O)(PPh_3)_2$ (**6a**). We conclude that the driving force for isomerization in $\mathbf{5^F}$ is minimized by the electron deficiency of the perfluorophenoxide ring. In contrast, incorporation of the aryloxide entity within a chelating framework proves insufficient to inhibit isomerization. Thus, reaction of **4a** or $RuCl_2(PPh_3)_3$ (**4b**) with the sodium salt of 2′-(diphenylphosphino)-1,1′-binaphthyl-2-ol (NaO-MOP) yields RuX(O-MOP)(PPh_3) (**7a**, X = H; **7b**, X = Cl). Detailed 1- and 2-D NMR analysis of **7b** provides unequivocal evidence that the O-MOP ligand is bound to Ru in a σ fashion through phosphorus and in a π fashion via the aryloxide ring. The crystal structure of $\mathbf{5^F}$·THF is reported.

Introduction

Robust "pseudohalide" ligands based on the phenoxide ion offer considerable promise as sterically and electronically tunable anionic donors in transition-metal catalysis. In the area of olefin metathesis, remarkable selectivities have been achieved in asymmetric ring-closing metathesis (RCM) using group 6 complexes of biphenolate and binaphtholate ligands (e.g. **1**; Chart 1).[1,2] Within the more robust ruthenium catalysts, impressive selectivity was reported for complexes containing a binaphtholate-derived ligand (e.g. **2**),[3,4] while our own group recently described exceptionally high turnover numbers (>40 000) in RCM via perfluorophenoxide derivative **3**, the first long-lived Ru−pseudohalide catalyst for olefin metathesis.[5]

A stable ligand architecture can be critical in determining catalyst lifetime and selectivity and, ultimately, catalyst utility. Several important calorimetric and reactivity studies[6−9] have led to reevaluation of the assumption that late-transition-metal−oxygen bond energies are inherently low, as the Pearson "hard−soft" formalism would suggest. Recent work from our group,[10] however, suggests that the well-established stability of the Ru−OAr bond within complexes of the type[6] $Ru(\sigma\text{-}OAr)_2(PMe_3)_4$ may be a function of the nonlability of the ancillary ligands. Thus, related complexes containing *labile* PPh_3 groups (e.g. $RuCl(\sigma\text{-}OAr)(PPh_3)_3$, $RuH(\sigma\text{-}OAr)(PPh_3)_3$; Ar = Ph, *p*-^{t}Bu$C_6H_4$) are not isolable, but undergo facile $\sigma \rightarrow \pi$ isomerization, enabled by loss of phosphine, to generate π-aryloxide derivatives (e.g. **6**, Scheme 1).[10−12] We speculated that the stability of the Ru(σ-OAr) bond in **3** could arise from the attenuated π-donor capacity of the perfluorophe-

Chart 1

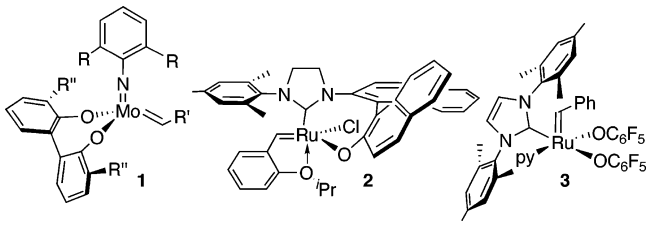

---

* To whom correspondence should be addressed. E-mail: dfogg@science.uottawa.ca. Fax: (613) 562-5170.

(1) Hoveyda, A. H.; Schrock, R. R. *Chem. Eur. J.* **2001**, *7*, 945.
(2) Tsang, W. C. P.; Hultzsch, K. C.; Alexander, J. B.; Bonitatebus, P. J.; Schrock, R. R.; Hoveyda, A. H. *J. Am. Chem. Soc.* **2003**, *125*, 2652.
(3) Van Veldhuizen, J. J.; Garber, S. B.; Kingsbury, J. S.; Hoveyda, A. H. *J. Am. Chem. Soc.* **2002**, *124*, 4954.
(4) Van Veldhuizen, J. J.; Gillingham, D. G.; Garber, S. B.; Kataoka, O.; Hoveyda, A. H. *J. Am. Chem. Soc.* **2003**, *125*, 12502.
(5) Conrad, J. C.; Amoroso, D.; Czechura, P.; Yap, G. P. A.; Fogg, D. E. *Organometallics* **2003**, *22*, 3634.
(6) Fulton, J. R.; Holland, A. W.; Fox, D. J.; Bergman, R. G. *Acc. Chem. Res.* **2002**, *35*, 44.
(7) Bryndza, H. E.; Tam, W. *Chem. Rev.* **1988**, *88*, 1163.
(8) Holland, P. L.; Andersen, R. A.; Bergman, R. G.; Huang, J.; Nolan, S. P. *J. Am. Chem. Soc.* **1997**, *119*, 12800.
(9) Huang, J.; Li, C.; Nolan, S. P.; Petersen, J. L. *Organometallics* **1998**, *17*, 3516.
(10) Snelgrove, J. L.; Conrad, J. C.; Yap, G. P. A.; Fogg, D. E. *Inorg. Chim. Acta* **2003**, *345*, 268.
(11) Other examples of such behavior in Ru chemistry include the formation of $RuH(\pi\text{-}ArO)(PR_3)_2$ by reaction of phenols with $RuH_2(PPh_3)_4$, $RuH_2(H_2)_2(PCy_3)_2$, or $RuH(C_6H_4PPh_2)(PPh_3)_2(Et_2O)$, and of $Ru(\pi\text{-}ArO)L_3^{n+}$ (n = 1, L_3 = arene; n = 0, L_3 = Cp*) by reaction of phenols or phenoxides with $[RuCl(\pi\text{-arene})]_2(\mu\text{-}Cl)_2$, $[Cp^*Ru(OMe)]_2$, or $[Cp^*Ru(\mu\text{-}Cl)]_4$. See: (a) Cole-Hamilton, D. J.; Young, R. J.; Wilkinson, G. *J. Chem. Soc., Dalton Trans.* **1976**, 1995. (b) Rosete, R. O.; Cole-Hamilton, D. J.; Wilkinson, G. *J. Chem. Soc., Dalton Trans.* **1979**, 1618. (c) Christ, M. L.; Sabo-Etienne, S.; Chung, G.; Chaudret, B. *Inorg. Chem.* **1994**, *33*, 5316. (d) Cole-Hamilton, D. J.; Wilkinson, G. *New J. Chem.* **1977**, *1*, 141. (e) Bennett, M. A.; Matheson, T. W. *J. Organomet. Chem.* **1979**, *175*, 87. (f) Bücken, K.; Koelle, U.; Pasch, R.; Ganter, B. *Organometallics* **1996**, *15*, 3095. (g) Chaudret, B.; Xiaodong, H.; Huang, Y. *J. Chem. Soc., Chem. Commun.* **1989**, 1844. (h) Koelle, U.; Wang, M. H.; Raabe, G. *Organometallics* **1991**, *10*, 2573. (i) Loren, S. D.; Campion, B. K.; Heyn, R. H.; Tilley, T. D.; Bursten, B. E.; Luth, K. W. *J. Am. Chem. Soc.* **1989**, *111*, 4712.

10.1021/om049394j CCC: $30.25
Publication on Web 12/08/2004

Scheme 1

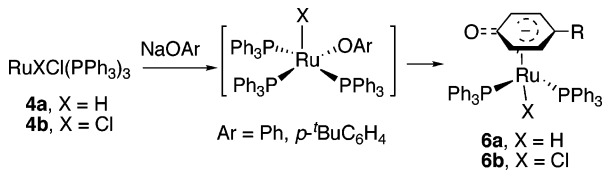

Scheme 2

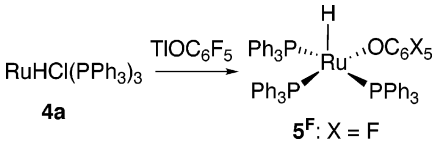

noxide ring,[13] while the chelate effect might be responsible for the stability of **2**. With the intention of clarifying these issues via direct comparison with the systems already examined, we undertook reaction of the labile precursors **4** with perfluorophenoxide anion and with the heterobifunctional phosphine−binaphtholate ligand NaO-MOP (sodium 2′-(diphenylphosphino)-2-oxy-1,1′-binaphthyl).

Results and Discussion

Treatment of a THF solution of $RuHCl(PPh_3)_3$ (**4a**) with thallium pentafluorophenoxide effected complete conversion to the σ-aryloxide complex $\mathbf{5^F}$ within 3 h at 22 °C (Scheme 2).[14] In contrast with the corresponding protio-phenoxide species $RuH(OC_6H_5)(PPh_3)_3$ ($\mathbf{5^H}$), complex $\mathbf{5^F}$ shows no tendency to isomerize. The red product was isolated in ca. 80% yield, and NMR and combustion analysis are consistent with formulation of the complex as $RuH(OC_6F_5)(PPh_3)_3$. Room-temperature $^{31}P\{^1H\}$ NMR analysis reveals a broad singlet centered at 47 ppm, which resolves into an A_2B pattern at −50 °C (δ_P 87.1 (t, 1P), 40.9 (d, 2P); $^2J_{PP} = 26$ Hz), confirming retention of all three triphenylphosphine ligands. The hydride signal is observed as a quartet of triplets, split by long-range coupling to two ^{19}F nuclei, as well as the expected two-bond coupling to phosphorus (δ_H −22.3 ppm; $^2J_{PH} = 27.9$ Hz, $^5J_{FH} = 7.2$ Hz).[15] The coupling assignments are supported by $^1H\{^{19}F\}$ and $^1H\{^{31}P\}$ NMR experiments, which reveal the hydride signal as a quartet and a triplet, respectively.

^{19}F NMR analysis of $\mathbf{5^F}$ reveals signals at chemical shifts similar to those found for the σ-OAr ligand within **3**, consistent with σ-coordination of the aryloxide ring (Table 1). A comparable range is found for the ^{19}F nuclei within free perfluorophenol, as well as thallium perfluorophenoxide. In comparison, signals for the *π-bound* perfluoroaryloxy ring in $[CpRu(\eta^5\text{-}C_6F_5O)]$ or $[CpRu(\eta^6\text{-}C_6F_5OH)]^+$ are found 20−30 ppm upfield.[13a,16] The coordination mode of the aryloxide ligand within $\mathbf{5^F}$ is confirmed by X-ray analysis of crystals obtained by slow evaporation of a concentrated THF solution. An ORTEP diagram, with relevant bond lengths and angles, is shown in Figure 1.

Table 1. $^{19}F\{^1H\}$ NMR Values for Perfluorophenol and Its Metal Complexes

compd	solvent	δ_F (ppm)	ref
C_6F_5OH	$CDCl_3$	−87.7 to −88.1 (m, 4F) −92.1 to −92.6 (m, 1F)	this work[a]
$TlOC_6F_5$	$CDCl_3$[b]	−81.8 to −84.1 (m, 2F) −88.55 (m, 2F) −99.65 (m, 1F)	this work[a]
$Ru(\sigma\text{-}OC_6F_5)_2$(IMes)-(py)(CHPh) (**3**)	$CDCl_3$	−86.45 (m, 2F) −86.7 (m, 2F) −94.27 (m, 2F) −94.50 (m, 2F) −104.8 to −106.0 (m, 2F)	5
$RuH(\sigma\text{-}OC_6F_5)$-$(PPh_3)_3$ ($\mathbf{5^F}$)	C_6D_6	−93.6 (m, 2 F) −94.7 to −94.9 (m, 2F) −107.8 (m, 1F)	this work[a]
$[Cp^*Ru(\eta^5\text{-}C_6F_5O)]$	$CDCl_3$	−108.4 (m, 2F) −112.3 (m, 2F) −119.0 (m, 1F)	13a, 16
$[Cp^*Ru(\eta^6\text{-}C_6F_5OH)]^+$	$CDCl_3$	−98.4 (m, 2F) −100.6 (m, 2F) −103.6 (m, 1F)	13a, 16

[a] ^{19}F NMR spectra measured at 282 MHz, 298 K, reported relative to trifluoroacetic acid at 0 ppm; the patterns show second-order effects. [b] The values in C_6D_6 are rather similar (−84.41 (m, 2F), −90.16 (m, 2F), −101.83 (m, 1F)), with limited perturbation by π-stacking[17] interactions.

Having confirmed the efficacy of electronic parameters in determining the coordination mode of the aryloxide entity, we turned our attention to the possibility that incorporating an aryloxy group within a chelating framework can likewise prevent isomerization. An attractive candidate for exploration is the chiral phosphine auxiliary "HO-MOP" (2′-(diphenylphosphino)-1,1′-binaphthyl-2-ol), a rare bidentate member of the monophosphine or MOP family of binaphthol-derived ligands developed by Hayashi et al.[18,19] We prepared racemic HO-MOP in 82% yield from binaphthol: in a minor modification of the literature route (Scheme 3),[18] we used trichlorosilane to reduce the phosphine oxide and to deprotect the triflate in a single step.

The HO-MOP ligand is readily converted into its sodium salt by reaction with Na_2CO_3. Subsequent reaction with **4a** or **4b** in CH_2Cl_2 affords orange RuX(O-MOP)(PPh_3) (X = H, **7a**; X = Cl, **7b**; Scheme 4) within 24 h at 22 °C. Strong evidence for the proposed formulation is provided by inert-atmosphere MALDI

(12) While of limited utility for olefin metathesis, such π-aryloxide species are of interest as catalysts for asymmetric Diels−Alder reactions (see: Faller, J. W.; D'Alliessi, D. G. *Organometallics* **2003**, *22*, 2749. Faller, J. W.; Lavoie, A. R.; Grimmond, B. J. *Organometallics* **2002**, *21*, 1662) and are of potential relevance for nucleophilic phenol functionalization (see: Le Bras, J.; Amouri, H.; Vaissermann, J. *Inorg. Chem.* **1998**, *37*, 5056 and references therein) or carbonylation (see: Dockter, D. W.; Fanwick, P. E.; Kubiak, C. P. *J. Am. Chem. Soc.* **1996**, *118*, 4846. Rees, W. M.; Churchill, M. R.; Fettinger, J. C.; Atwood, J. D. *Organometallics* **1985**, *4*, 2179).

(13) Examples of π-bound fluorophenoxide have, however, been reported. See: (a) Koelle, U.; Hörnig, A.; Englert, U. *Organometallics* **1994**, *13*, 4064. (b) Curnow, O. J.; Hughes, R. P. *J. Am. Chem. Soc.* **1992**, *114*, 5895.

(14) Similar behavior is observed with sodium pentafluorophenoxide, but the reaction is only ca. 30% complete at 3 h (100% at 48 h). The accelerating effect of Ag^+ and Tl^+ salts in halide substitution of metal complexes has been attributed to electrophilic "pull" by the heavy-metal cations, possibly via direct electrophilic attack on the halogen atom. See: Danopoulos, A. A.; Wilkinson, G.; Sweet, T. K. N.; Hursthouse, M. B. *Polyhedron* **1994**, *13*, 2899.

(15) The $^5J_{PF}$ coupling is too small to observe in the $^{31}P\{^1H\}$ NMR spectrum.

(16) Literature values, originally reported relative to $CFCl_3$, are cited relative to trifluoroacetic acid at 0 ppm.

(17) Williams, J. H. *Acc. Chem. Res.* **1993**, *26*, 593.

(18) Uozumi, Y.; Tanahashi, A.; Lee, S. Y.; Hayashi, T. *J. Org. Chem.* **1993**, *58*, 1945.

(19) Hayashi, T. *Acc. Chem. Res.* **2000**, *33*, 354.

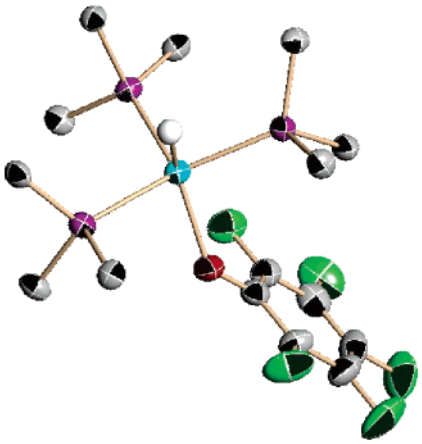

Figure 1. ORTEP representation of $RuH(\sigma\text{-}OC_6F_5)(PPh_3)_3$ (**5^F**) with thermal ellipsoids at the 30% probability level. Phenyl groups are represented by their ipso carbon atoms, and the THF solvate is omitted for clarity. Selected bond distances (Å) and angles (deg): Ru−O1 = 2.1350(17), Ru−P1 = 2.2242(6), Ru−P3 = 2.3389(7), Ru−P2 = 2.3911(7), Ru−H1 = 1.49(3), O1−C6 = 1.311(3); O1−Ru−P1 = 135.23(6), O1−Ru−P3 = 94.91(5), P1−Ru−P3 = 99.22(3), O1−Ru−P2 = 85.40(5), P1−Ru−P2 = 98.42(3), P3−Ru−P2 = 154.40(2), H1−Ru−P1 = 86(1), H1−Ru−P2 = 82(1), H1−Ru−P3 = 81(1), H1−Ru−O1 = 138(1), C6−O1−Ru = 135.80(15).

Scheme 3

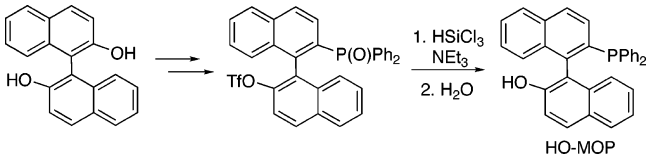

Scheme 4

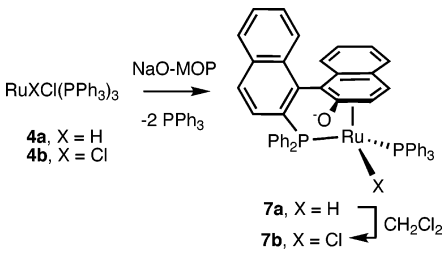

mass spectrometric analysis. For both **7a** and **7b**, a peak-for-peak correspondence is found between the simulated and observed isotope patterns for the molecular ions (Figure 2). The complexity of these patterns—a function of the presence of seven naturally occurring isotopes of ruthenium and (in **7b**) two isotopes of chlorine—provides powerful insight into the molecular composition. Critical to their observation is use of a matrix that ionizes by charge transfer, rather than protonation.[20]

^{31}P NMR spectra of **7a** and **7b** show well-resolved AB systems (**7a**, δ 63.1, 56.3, $^2J_{PP}$ = 25 Hz; **7b**, δ 49.9, 46.9, $^2J_{PP}$ = 58 Hz), accompanied, in the case of **7a**, by a hydride triplet (−11.84 ppm, $^2J_{PH}$ = 34 Hz) in the ^{1}H NMR spectrum. Isolation of **7a** was complicated by solvent-induced chlorination of the hydride ligand to generate **7b** (Scheme 4), as indicated by ^{31}P NMR

(20) Eelman, M. D.; Moriarty, M. M.; Fogg, D. E. Manuscript in preparation.

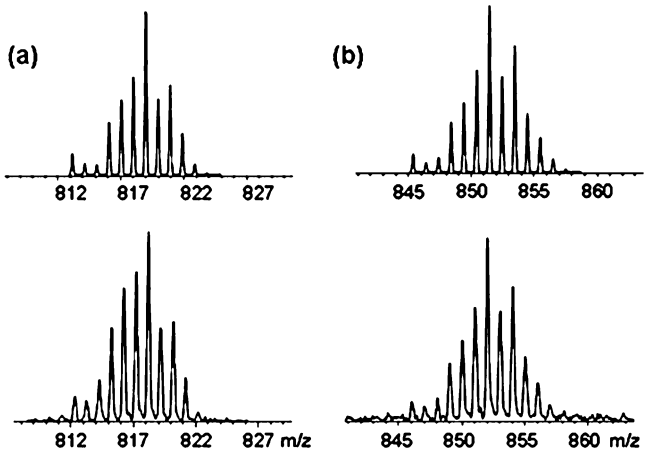

Figure 2. MALDI-MS spectra (anthracene matrix), showing simulated (top) and observed (bottom) isotope patterns for $M^{+\cdot}$ within (a) **7a** (observed *m/z* 818.3, calculated *m/z* 818.1); (b) **7b** (observed *m/z* 852.0, calculated *m/z* 852.1).

Chart 2. Reported (A−F) and Proposed (7) Coordination Modes for Binap and Related MOP Ligands

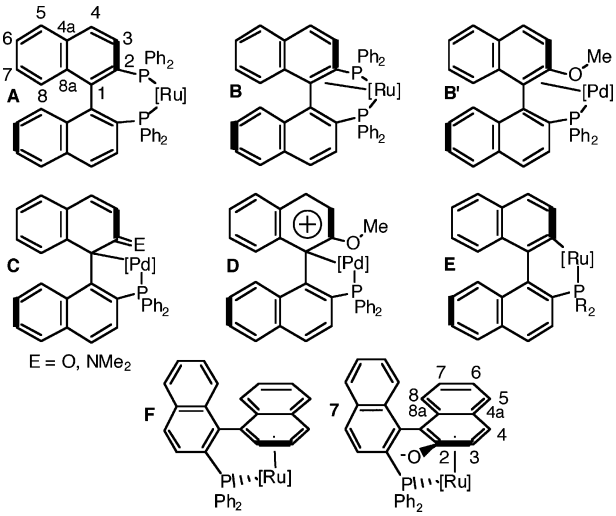

analysis. Attempts to circumvent this behavior by carrying out the reaction in THF resulted in complex mixtures, as we previously noted in the corresponding phenoxide chemistry,[10] while reactions in benzene did not proceed to completion. Subsequent experiments therefore targeted isolation and characterization of **7b**. We obtained the latter light orange complex in ca. 90% yield, following chromatography to remove traces of an unknown byproduct (δ_P 52 ppm, s). The stability of **7b** to aerobic chromatography is noteworthy. NMR samples in C_6D_6 or $CDCl_3$ likewise show no evidence of decomposition in air for up to 3 days at room temperature, and the complex also fails to react with sterically undemanding donors such as CO and MeCN. All of these features point toward a nonlabile, coordinatively saturated structure.

While binap is conventionally considered a simple κ^2-PP donor (see **A**, Chart 2), a wealth of alternative coordination modes (**B**−**F**) has been established for binap and related MOP ligands in a series of elegant NMR and X-ray crystallographic studies.[21−32] ^{1}H NMR analysis of **7b** indicates the presence of a π-bound ring: while most of the naphthyl protons appear in the

aromatic region, two sets of doublets of doublets, each integrating to 1H, are found further upfield (δ_H 4.50, $^3J_{HH}$ = 7.4 Hz, $^3J_{HP}$ = 3.9 Hz; δ_H 6.01, $^3J_{HH}$ = 7.4 Hz, $^3J_{HP}$ = 2.5 Hz). Both signals collapse to doublets on ^{31}P decoupling. These protons couple (TOCSY, COSY) to each other but to no other ^{1}H nuclei, supporting assignment to H3 and H4, respectively, of the π-bound naphthol ring.[33] As the multiplicity suggests, each couples to a *single* ^{31}P nucleus: ^{1}H−^{31}P HMQC analysis confirms that the signal for H3 (4.50 ppm) correlates strongly only with the ^{31}P NMR signal for PPh_3 (46.9 ppm) and that for H4 (6.01 ppm) only with the ^{31}P NMR signal for the O-MOP phosphorus (49.9 ppm).[34] This implies a dihedral angle of ca. 90° between H3 and the O-MOP phosphorus and between H4 and *P*Ph_3. Consistent with this is the geometry shown for **7** in Scheme 4, with an anti disposition of the PPh_3 ligand and the aryloxy oxygen.[35] Each of the protons H3 and H4 also correlates with an upfield ^{13}C{^{1}H} NMR doublet (C3, δ_C 97.3, $^2J_{CP}$ = 10.0 Hz; C4, δ_C 94.7, $^2J_{CP}$ = 8.9 Hz; ^{1}H−^{13}C HMQC) that collapses to a singlet on simultaneous ^{31}P and ^{1}H decoupling. While the absence of two $^2J_{CP}$ couplings for C3 and C4 is unexpected, similar multiplicities are reported for related piano-stool complexes of type **F**, in which two phosphine donors are present.[22,26,29,30]

^{13}C NMR analysis is invaluable in establishing the hapticity of π-bound aromatic rings. Table 2 summarizes the ^{13}C NMR chemical shifts for the σ,π-bound ring in **7b** and the reported complexes of Chart 2. Of particular interest among the latter is Pd(acac)(κ^1: κ^1-O-MOP) (**8**), a complex of class **C** recently reported by Pregosin, Albinati, and co-workers.[28] NMR and X-ray analysis revealed that the binaphthol ring in **8** is bound via C1 and that the C−O bond has significant ketonic character. Notably, the "phenolic" carbon C2 gives rise to a ^{13}C NMR signal at 194 ppm, a location characteristic of the carbonyl carbon in α,β-unsaturated ketones. In contrast, the corresponding carbon signal for **7b** appears at 155.6 ppm, very near the value of 151 ppm found for the free ligand. The remaining quaternary carbon signals of the π-bound ring are readily assigned on the basis of their upfield location, their disappearance on DEPT-135 analysis, and the couplings revealed by a ^{1}H−^{13}C HMBC experiment[36] (Figure 3). The HMBC correlations, reinforced by ^{1}H−^{1}H TOCSY analysis (Figure 4), as well as HMQC experiments, enable full assignment of the remaining ^{13}C and ^{1}H nuclei in the naphthol ring: all signals, with the exception of that for C1, due to the "aryloxy" ring appear at considerably lower chemical shifts than they do in **8** (Table 2). Indeed, a closer resemblance exists between **7** and the κ^1: η^6 structure **F**, numerous examples of which have now been reported.[22,24,25,29−32]

Table 2. ^{13}C NMR Chemical Shifts (ppm) for the σ,π-Bound Ring in 7b and Related Complexes[a]

	7b	**B**,[21−26] **B′** [27]	**C**[b,28]	**D**[28]	**E**[26]	**F**[22,24,25,29−32]
C1	83.0	87−101	70.5	87	140−141	92−120
C2	155.6	55−73	193.7	166	171−174	73−101
C3	97.3	125−127	127.6	113	136	100−108
C4	94.7	138.3	142.8	147	123	89−109
C4a	112.6	142−145	146.1	140	133	107−121
C8a	103.5	130−133	128.8	129	131	110−118

[a] For numbering, see Chart 2. [b] Values tabulated for E = O only.

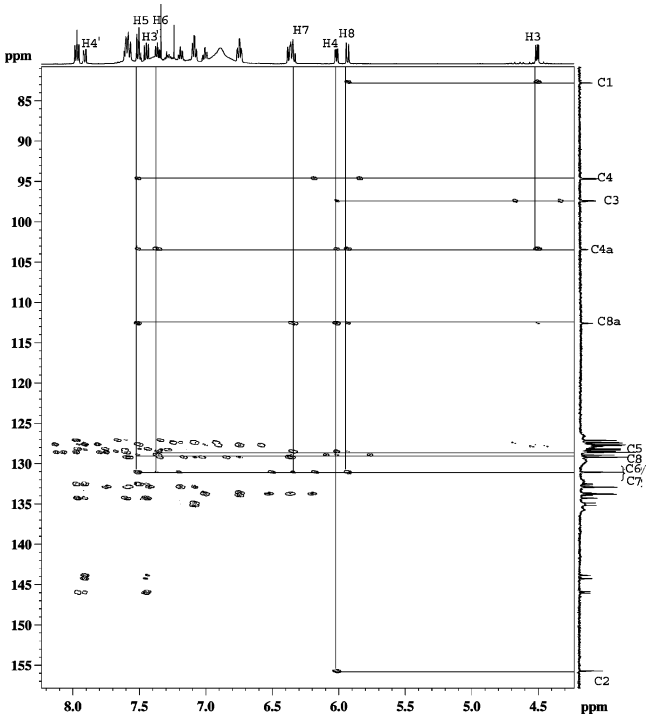

Figure 3. ^{1}H−^{13}C HMBC NMR spectrum for **7b** (500 MHz, 298 K, $CDCl_3$).

(21) Feiken, N.; Pregosin, P. S.; Trabesinger, G.; Albinati, A.; Evoli, G. L. *Organometallics* **1997**, *16*, 5756.
(22) den Reijer, C. J.; Woerle, M.; Pregosin, P. S. *Organometallics* **2000**, *19*, 309.
(23) den Reijer, C. J.; Dotta, P.; Pregosin, P. S.; Albinati, A. *Can. J. Chem.* **2001**, *79*, 693.
(24) Geldbach, T. J.; Pregosin, P. S.; Albinati, A.; Rominger, F. *Organometallics* **2001**, *20*, 1932.
(25) Geldbach, T. J.; Pregosin, P. S. *Eur. J. Inorg. Chem.* **2002**, 1907.
(26) Geldbach, T. J.; Pregosin, P. S.; Albinati, A. *Organometallics* **2003**, *22*, 1443.
(27) Lloyd-Jones, G. C.; Stephen, S. C.; Murray, M.; Butts, C. P.; Vyskocil, S.; Kocovsky, P. *Chem. Eur. J.* **2000**, *6*, 4348.
(28) Dotta, P.; Kumar, P. G. A.; Pregosin, P. S.; Albinati, A.; Rizzato, S. *Organometallics* **2003**, *22*, 5345.
(29) Geldbach, T. J.; Drago, D.; Pregosin, P. S. *Chem. Commun.* **2000**, 1629.
(30) Geldbach, T. J.; Pregosin, P. S.; Bassetti, M. *Organometallics* **2001**, *20*, 2990.
(31) Hermatschweiler, R.; Pregosin, P. S.; Albinati, A.; Rizzato, S. *Inorg. Chim. Acta* **2003**, *354*, 90.
(32) Geldbach, T. J.; Breher, F.; Gramlich, V.; Kumar, P. G. A.; Pregosin, P. S. *Inorg. Chem.* **2004**, *43*, 1920.
(33) While the corresponding protons (H3′, H4′) of the phosphorus-functionalized ring will give rise to an identical set of COSY correlations and would likewise be shifted upfield if this ring were π-bound, the PPh_2 group would then result in a ^{31}P NMR signal near 0 ppm.[25] (The signals for H3′ and H4′, located from the TOCSY and COSY NMR spectra, in fact appear at 7.45 ppm (H3′: dd, $^3J_{HH}$ = 8.5 Hz; $^3J_{HP}$ = 6.9 Hz) and 7.91 ppm (H4′: dd, $^3J_{HH}$ = 8.6 Hz; $^4J_{HP}$ = 1.5 Hz); they are distinguished on the basis of the magnitude of their respective J_{HP} values. We distinguish between the signals for H3 and H4, in turn, on the basis of the number and identity of $^3J_{HC}$ correlations revealed in HMBC experiments. For further details, see the Supporting Information.
(34) Assignment of the ^{31}P NMR signals is made on the basis of the coupling of the O-MOP phosphorus to H3′ and H4′.
(35) This geometry permits an incipient interaction between the oxygen and phosphorus O-MOP substituents, a feature that may account for the diastereomeric bias in formation of **7b** (vide infra).
(36) It will be noted that three of the anticipated $^2J_{HC}$ correlations (those between H3, C2, and C4 and between H6 and C7) are missing from the HMBC spectrum. Owing to the small size of the $^2J_{HC}$ coupling constants in aromatic rings (often on the order of 1 Hz), these correlations are generally less reliable than the corresponding $^3J_{HC}$ couplings, for which values of 5−10 Hz are typical (see: Kalinowski, H.-O.; Berger, S.; Braun, S. *Carbon-13 NMR Spectroscopy*; Wiley: Toronto, 1988) The chemical shift and the TOCSY, HMQC, and $^3J_{HC}$ HMBC correlations for the ^{1}H NMR signal at 4.50 ppm are uniquely consistent with assignment to H3.

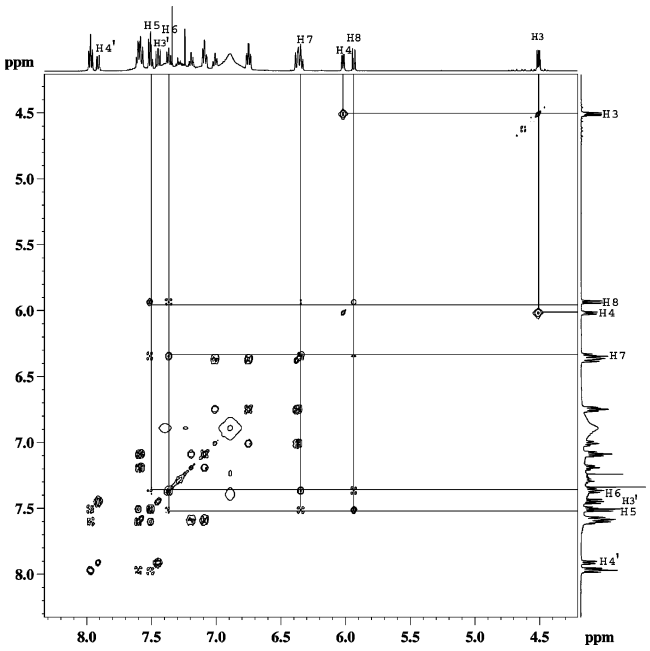

Figure 4. ^{1}H−^{1}H TOCSY spectrum of **7b** (500 MHz, 298 K, $CDCl_3$).

Coordination of "tethered" binaphthyl and biphenyl ligands within a piano-stool structure can give rise to diastereomers, if a sterogenic metal center is present. We observe only one AB pattern in the ^{31}P NMR spectrum of **7b**, however, even at −90 °C, suggesting the presence of a single diastereomer. (We exclude the possibility of rapid epimerization of the metal center, given the nonlability of the phosphine ligand in reactions with donors such as carbon monoxide and acetonitrile; vide supra.) While Faller has described biphenyl complexes in which unfavorable steric interactions between the bulky PPh_3 ligand and a dimethylamino ring substituent dictate formation of a single diastereomer,[37] the limited bulk of the O-MOP oxygen in **7b** should minimize such effects. The observed diastereomeric bias may instead arise from a *favorable* interaction between the PPh_3 ligand and the O-MOP oxygen.

Conclusions

The retention in $\mathbf{5^F}$ of a stable, σ-bonded perfluorophenoxide and three labile PPh_3 ligands contrasts with the instability of the corresponding phenoxide derivatives, which undergo rapid isomerization, with loss of PPh_3, to yield π-OAr complexes of type **6**.[10] From this difference in behavior, we suggest that the electron deficiency of the aryloxide ring is a key factor contributing to the stability of the Ru(σ-OAr) entity within complexes such as $\mathbf{5^F}$ and **3**. In contrast, the binaphthol-derived O-MOP ligand in **7** is bound in a σ fashion through phosphorus and in a π fashion via the η^6-aryloxide ring. Chelation thus appears insufficient to inhibit σ → π isomerization of the Ru−OAr unit, where the lability of the ancillary ligands in the precursor complex is sufficient to liberate the three coordination sites required to bind the phenolic ring.

The broader significance of these findings lies in their implications for the deployment of chelating aryloxide ligands in late-transition-metal catalysts. In context of the findings above, the apparent stability of the Hoveyda complex[3,4] **2** to σ → π isomerization is of considerable interest. We speculate that this may in fact reflect the rather low lability of the dative Ru−O(ether) bond (as indeed implied by the chromatographic stability and the slow initiation of **2**[3]). The *active* catalyst, generated by metathetical exchange of the chelating alkylidene, is coordinatively unsaturated and may thus be unstable toward σ → π isomerization. Indeed, derivatives of **2** modified to destabilize the ether chelate appear to decompose much more readily.[4] Conversely, the electron deficiency of the perfluorophenoxide ligand in complex **3**, which disfavors isomerization, is presumably a key factor in the remarkable lifetime of this catalyst.

Experimental Section

General Procedures. All reactions were carried out at room temperature (22 °C) under N_2 using standard Schlenk or drybox techniques, unless stated otherwise. Dry, oxygen-free solvents were obtained using an Anhydrous Engineering solvent purification system and stored over Linde 4 Å molecular sieves. $CDCl_3$ and C_6D_6 were dried over activated sieves (Linde 4 Å) and degassed by consecutive freeze/pump/thaw cycles. $RuHCl(PPh_3)_3$ (**4a**) and $RuCl_2(PPh_3)_3$ (**4b**) were prepared as previously described.[38−40] (±)-2′-(Diphenylphosphino)-2-(((trifluoromethyl)sulfonyl)oxy)-1,1′-binaphthyl was prepared over two steps from racemic binaphthol according to the literature procedure.[18] ^{1}H NMR (300 or 500 MHz), ^{31}P NMR (121 or 202 MHz), ^{19}F NMR (282 MHz), and ^{13}C NMR (75 or 125 MHz) spectra were recorded on a Bruker Avance-300, Avance-500, or AMX-500 spectrometer. NMR spectra are reported relative to external 85% H_3PO_4 (^{31}P), trifluoroacetic acid (^{19}F), or TMS (^{1}H, ^{13}C) at 0 ppm. Variable temperature, 2-D, and selective decoupling NMR experiments were carried out on the Bruker AMX-500 and Bruker Avance-500 instruments, the latter being equipped with a triple-resonance probe. IR spectra were measured on a Bomem MB100 IR spectrometer. Inert-atmosphere MALDI-MS analyses were performed using a Bruker OmniFlex MALDI TOF mass spectrometer equipped with a nitrogen laser (337 nm) and interfaced to an MBraun Labmaster 130 glovebox. Data were collected in positive reflection mode, with the accelerating voltage held at 20 kV for all experiments. Matrix (anthracene) and analyte solutions were prepared in CH_2Cl_2 at concentrations of 20 and 1 mg/mL, respectively; samples were mixed in a matrix to analyte ratio of 20:1. Microanalyses were carried out by Guelph Chemical Laboratories Ltd., Guelph, Ontario, Canada.

Note! The toxicity of thallium (particularly in the +1 oxidation state) is well established, and the subject has been recently reviewed.[41] Care must be taken to prevent introduction into the body by inhalation, by ingestion via contaminated hands or gloves, or through the skin. All thallium reagents and wastes, including contaminated solvents, were handled using double-glove and secondary containment procedures, with separate disposal of all wastes in accordance with government regulations.

(±)-2′-(Diphenylphosphino)-1,1′-binaphthyl-2-ol (HO-MOP). In a modification of the literature route,[18] a solution of (±)-2′-(diphenylphosphino)-2-(((trifluoromethyl)sulfonyl)-oxy)-1,1′-binaphthyl (677.4 mg, 1.124 mmol) in 20 mL of toluene was treated with trichlorosilane (761 mg, 5.62

(37) Faller, J. W.; D'Alliessi, D. G. *Organometallics* **2003**, *22*, 2749.
(38) Amoroso, D.; Snelgrove, J. L.; Conrad, J. C.; Drouin, S. D.; Yap, G. P. A.; Fogg, D. E. *Adv. Synth. Catal.* **2002**, *344*, 757.
(39) Stephenson, T. A.; Wilkinson, G. *J. Inorg. Nucl. Chem.* **1966**, *28*, 945.
(40) Hallman, P. S.; Stephenson, T. A.; Wilkinson, G. *Inorg. Synth.* **1970**, *12*, 237.
(41) Galván-Arzate, S.; Santamaría, A. *Toxicol. Lett.* **1998**, *99*, 1.

mmol) and Et_3N (7 equiv). The solution was stirred at 100 °C for 16 h and then cooled, diluted with Et_2O, and quenched with saturated $NaHCO_3$. The resulting white gel was filtered through Celite, which was then washed with Et_2O (3 × 30 mL). The organic phase was dried over $MgSO_4$, concentrated, and chromatographed on silica gel (20% EtOAc/hexanes) to afford the product as a white solid. Yield: 409 mg (80%). NMR data are in good agreement with the reported values.[18] ^1H NMR (C_6D_6, 300 MHz): δ 8.22−6.42 (m, 22H, aromatic), 4.63 (br s, 1H, −O*H*). $^{31}P\{^1H\}$ NMR (C_6D_6, 121 MHz): δ −13.4 (s).

Sodium (±)-2′-(Diphenylphosphino)-2-oxy-1,1′-binaphthyl (NaO-MOP). Solid Na_2CO_3 (732 mg, 6.91 mmol) was added to a solution of HO-MOP (93.0 mg, 0.205 mmol) in 5 mL of CH_2Cl_2. The suspension was stirred at room temperature for 24 h and then filtered through Celite to remove $NaHCO_3$ and excess Na_2CO_3. The solvent was removed under vacuum to give the desired salt as a white solid. Yield: 87 mg (89%).

RuH(OC$_6$F$_5$)(PPh$_3$)$_3$ (5^F). Thallium pentafluorophenoxide (176 mg, 0.45 mmol) was added to a purple solution of $RuHCl(PPh_3)_3$ (**4a**; 420 mg, 0.45 mmol) in 20 mL of THF. The mixture was stirred for 3 h, over which time it turned red. The solvent was removed under reduced pressure, and the resulting oil was dissolved in benzene and filtered through Celite to remove TlCl. The filtrate was concentrated and treated with pentane to precipitate a red solid, which was filtered off. Yield after drying in vacuo: 392 mg (81%). Blocklike crystals suitable for X-ray analysis were grown by slow evaporation of a saturated THF solution. ^1H NMR (C_6D_6): δ 7.40−7.31 (m, 17H, Ar), 6.94−6.90 (m, 10H, Ar), 6.85−6.80 (m, 18H, Ar), −22.29 (q of t, $^2J_{PH}$ = 27.9 Hz, $^5J_{FH}$ = 7.2 Hz, 1H, Ru*H*). $^{31}P\{^1H\}$ NMR (298 K, C_6D_6): δ 47 (br s). $^{31}P\{^1H\}$ NMR (248 K, C_7D_8): δ 87.1 (t, $^2J_{PP}$ = 26 Hz, 1P), 40.9 (d, $^2J_{PP}$ = 26 Hz, 2P). $^{13}C\{^1H\}$ NMR (C_6D_6): δ 144.7−139.6 (m, O*C*$_6$F$_5$), 136.6−136.1 (m, Ph), 134.9−134.6 (m, Ph), 132.5 (d, J = 9.6 Hz, Ph), 129.2 (s, Ph). $^{19}F\{^1H\}$ NMR (282.4 MHz, C_6D_6): δ −93.6 (m, 2 F), −94.6 to −94.9 (m, 2F), −107.8 (m, 1F). $^{19}F\{^1H\}$ NMR (223 K, C_7D_8): δ −88.8 to −88.9 (m, 1F, F_o), −92.01 (t, $^2J_{FF}$ = 20.9 Hz, 1F, F_m), −93.38 (t, $^2J_{FF}$ = 22.0 Hz, 1F, F_m), −102.5 to −102.6 (m, 1F, F_o), −106.9 to −107.0 (m, 1F, F_p). A low-temperature $^{19}F-^{19}F$ COSY experiment shows the following correlations (ppm): −89 and −93; −92 and −102; −92 and −107; −93 and −107. IR (Nujol): ν(Ru−H) 2089 cm^{-1}. Anal. Calcd for $RuC_{60}H_{46}P_3OF_5$: C, 67.22; H, 4.33. Found: C, 66.88; H, 4.05.

RuH(O-MOP)(PPh$_3$) (7a). $RuHCl(PPh_3)_3$ (**4a**; 50.1 mg, 0.0541 mmol), HO-MOP (26.2 mg, 0.0571 mmol), and Na_2CO_3 (143 mg, 1.35 mmol) were added to 2 mL of $CDCl_3$ and stirred for 24 h at room temperature. In situ ^{31}P NMR analysis showed signals for **7a** and **7b**. The corresponding reaction using NaO-MOP in C_6D_6 showed considerable residual starting material, probably owing to the limited solubility of the NaO-MOP salt; in THF, multiple products were evident. ^1H NMR ($CDCl_3$): δ −11.84 (t, $^2J_{PH}$ = 34 Hz, 1H, Ru*H*). $^{31}P\{^1H\}$ NMR ($CDCl_3$; peaks given for **7a** only): δ 63.1 (d, $^2J_{PP}$ = 25 Hz, 1P), 56.3 (d, $^2J_{PP}$ = 25 Hz, 1P). MALDI-MS, *m/z* found, 818.3; *m/z* calcd for $[M]^{\bullet+}$, 818.1.

RuCl(O-MOP)(PPh$_3$) (7b). To a solution of $RuCl_2(PPh_3)_3$ (**4b**; 106.0 mg, 0.111 mmol) in CH_2Cl_2 (4 mL) was added a solution of NaO-MOP (52.7 mg, 0.111 mmol) in 3 mL of CH_2Cl_2. The solution was stirred for 24 h, following which the solvent was removed, the residue redissolved in C_6H_6 and filtered (Celite), and the filtrate concentrated and treated with pentane to precipitate the product. Chromatography on silica gel (EtOAc eluant; crude product dissolved in 0.5 mL of CH_2Cl_2) and reprecipitation from benzene/hexanes, followed by washing with hexanes, afforded the orange product. Yield: 86 mg (91%). $^{31}P\{^1H\}$ NMR ($CDCl_3$, 121 MHz): δ 49.9 (d, $^2J_{PP}$ = 58 Hz, 1P), 46.9 (d, $^2J_{PP}$ = 58 Hz, 1P). ^1H NMR ($CDCl_3$, 500 MHz): δ 7.97 (t, $^3J_{HH}$ = 7.3 Hz, 2H, Ph), 7.91 (dd, $^3J_{HH}$ = 8.6 Hz; $^4J_{HP}$ = 1.5 Hz, 1H, H4′), 7.62−7.52 (m, 4H, Ph), 7.51 (d, $^3J_{HH}$ = 7.4 Hz, 1H, *H5*), 7.51−7.49 (m, 1H, Ph; overlaps with H5), 7.45 (dd, $^3J_{HH}$ = 8.5 Hz; $^3J_{HP}$ = 6.9 Hz, 1H, H3′), 7.42−7.37 (m, 3H, Ph), 7.37 (t, $^3J_{HH}$ = 7.6 Hz, 1H, *H6*), 7.35−6.74 (m, 17H, Ph), 6.38−6.34 (m, 2H, Ph; overlaps with H7), 6.34 (t, $^3J_{HH}$ = 8.4 Hz, 1H, *H7*), 6.01 (dd, $^3J_{HH}$ = 7.4 Hz; $^3J_{HP}$ = 2.5 Hz, 1H, *H4*), 5.93 (d, $^3J_{HH}$ = 8.5 Hz, 1H, *H8*), 4.50 (dd, $^3J_{HH}$ = 7.4 Hz, $^3J_{HP}$ = 3.9 Hz, 1H, *H3*). $^{13}C\{^1H\}$ NMR ($CDCl_3$, 125 MHz): δ 155.6 (s, *C2*), 133.8 (d, $^2J_{CP}$ = 10.0 Hz), 133.7 (s), 133.0 (d, $^2J_{CP}$ = 11.3 Hz), 131.1 (s, *C6* + *C7*), 128.9 (s, *C8*), 128.5 (s, *C5*), 112.6 (s, *C8a*), 103.5 (s, *C4a*), 97.3 (d, $^2J_{CP}$ = 10.0 Hz, *C3*), 94.7 (d, $^2J_{CP}$ = 8.9 Hz, *C4*), 83.0 (s, *C1*). MALDI-MS: *m/z* found, 852.0; *m/z* calcd for $[M]^{\bullet+}$, 852.1. Anal. Calcd for RuCl(O-MOP)(PPh_3)·(hexane) ($C_{56}H_{51}ClOP_2Ru$): C, 71.67; H, 5.48. Found: C, 71.45; H, 5.25.

Table 3. Crystal Data and Structure Refinement Details for RuH(OC$_6$F$_5$)(PPh$_3$)$_3$·THF (5^F·THF)

empirical formula	$C_{64}H_{56}F_5O_2P_3Ru$
formula wt	1146.07
temp	203(2) K
wavelength	0.71073 Å
cryst syst, space group	monoclinic, $P2_1/n$
unit cell dimens	a = 12.773(2) Å b = 25.338(5) Å c = 17.282(3) Å β = 105.381(3)°
V	5392.9(17) Å^3
Z, calcd density	4, 1.411 g/cm^3
abs coeff	0.44 mm^{-1}
F(000)	2360
cryst size	0.20 × 0.10 × 0.05 mm
θ range for data collecn	1.46−28.65°
limiting indices	$-16 \le h \le 16$, $0 \le k \le 32$, $0 \le l \le 23$
no. of rflns collected/unique	37 344/12 027 (R(int) = 0.0441)
completeness to θ = 28.65°	86.7%
abs cor	semiempirical from equivalents
max and min transmissn	1.000000 and 0.626317
refinement method	full-matrix least squares on F^2
no. of data/restraints/params	12 027/0/635
goodness of fit on F^2	1.033
final R indices ($I > 2\sigma(I)$)	R1 = 0.0403,[a] wR2 = 0.1003[b]
R indices (all data)	R1 = 0.0561, wR2 = 0.1075
largest diff peak and hole	0.584 and −0.963 e Å^{-3}

[a] $R1 = \Sigma||F_o| - |F_c||/\Sigma|F_o|$, [b] $wR2 = [\Sigma w\delta^2/\Sigma wF_o^2]^{1/2}$.

Attempted Reaction of RuCl(O-MOP)(PPh$_3$) (7b) with CO and MeCN. A solution of **7b** (10.2 mg, 0.012 mmol) in 1 mL of C_6D_6 was freeze−thaw degassed (× 5) and stirred under CO (1 atm) or with MeCN (1 mL) under Ar. No change was evident by $^{31}P\{^1H\}$ NMR analysis after 24 h.

X-ray Crystallography. Details of the crystal data and structure refinement for **5^F**·THF are contained in Table 3. Crystals of **5^F** were mounted on a thin glass fiber using paraffin oil and cooled to the data collection temperature. Data were collected on a Bruker AXS SMART 1k CCD diffractometer using 0.3° ω scans at 0, 90, and 180° in ϕ. Initial unit-cell parameters were determined from 60 data frames collected at different sections of the Ewald sphere. Semiempirical absorption corrections based on equivalent reflections were applied.[42] Systematic absences in the diffraction data and unit-cell parameters were uniquely consistent with the space group $P2_1/n$. The structure was solved by direct methods, completed with difference Fourier syntheses, and refined with full-matrix least-squares procedures based on F^2. The hydride ligand, H(1), was located from the difference map. A cocrystallized THF molecule was found in the initial solution, severely disordered at an inversion center. The data were modified with the Squeeze bypass filter of PLATON[43] with 629.8 Å^3 solvent accessible volume and 99 electron count/cell consistent with the initial solution and noncrystallographic data. All nonhy-

(42) Blessing, R. *Acta Crystallogr.* **1995**, *A51*, 33.
(43) Spek, A. L. *Acta Crystallogr.* **1990**, *A46*, C34.

dride hydrogen atoms were treated as idealized contributions. All scattering factors are contained in the SHELXTL 6.12 program library.[44]

Acknowledgment. This work was supported by the Natural Sciences and Engineering Research Council of Canada, the Canada Foundation for Innovation, the Ontario Innovation Trust, and the Ontario Research and Development Corporation.

(44) Sheldrick, G. M. Bruker AXS, Madison, WI, 2001.

Supporting Information Available: Figures and tables giving crystallographic data for **5^{F}**·THF and detailed 2-D NMR spectra for **7b**. This material is available free of charge via the Internet at http://pubs.acs.org.

OM049394J